frontiers in Physics

BRIEF RESEARCH REPORT
published: 30 June 2021
doi: 10.3389/fphy.2021.694080

Suppression of Breast Cancer Cell Migration and Epithelial-Mesenchymal Transition by Atmospheric Pressure Plasma

Kijung Kim[1], *Jinseung Choung*[2], *Ung Hyun Ko*[2], *Ara Jung*[3], *Wonho Choe*[1,4], *Jennifer H. Shin*[2]* *and Bomi Gweon*[3]*

[1]Department of Physics, Korea Advanced Institute of Science and Technology (KAIST), Daejeon, South Korea, [2]Department of Mechanical Engineering, Daejeon, South Korea, [3]Department of Mechanical Engineering, Sejong University, Seoul, South Korea, [4]Department of Nuclear and Quantum Engineering, Daejeon, South Korea

Atmospheric pressure plasma (APP) has emerged rapidly as a potent tool for cancer therapy thanks to its multiple anti-cancer effects. Depending on the types, APP has been shown to induce necrosis, apoptosis, or senescence in cancer cells *in vitro* and reduce tumor size *in vivo*. While recent progress in plasma medicine has led to various hypotheses for the molecular mechanism of APP, the key effector in anti-cancer processes still remains elusive. In this study, we show that APP treatment on an invasive breast cancer cell line (MDA-MB-231) dramatically alters these cells' morphology and further suppresses migratory activity. In addition to the functional changes, epithelial to mesenchymal transition (EMT) markers, such as vimentin and alpha-smooth muscle actin (α-SMA), were found to be down-regulated in MDA-MB-231 by the APP treatment. As a result, APP treatment appears to impact the invasive nature of cancer cells, motivating the possible use of APP as a therapeutic tool to suppress cancer metastasis.

Keywords: plasma treatment, cancer metastasis, cell migratoin, epithelial-mesenchymal transition, cancer invasion

OPEN ACCESS

Edited by:
Antonio D'Angola,
University of Basilicata, Italy

Reviewed by:
Jun-Seok Oh,
Osaka City University, Japan
Xanthe Strudwick,
University of South Australia, Australia

***Correspondence:**
Bomi Gweon
bgweon@sejong.ac.kr
Jennifer H. Shin
j_shin@kaist.ac.kr

Specialty section:
This article was submitted to Plasma Physics, a section of the journal Frontiers in Physics

Received: *12 April 2021*
Accepted: *15 June 2021*
Published: *30 June 2021*

Citation:
Kim K, Choung J, Ko UH, Jung A, Choe W, Shin JH and Gweon B (2021) Suppression of Breast Cancer Cell Migration and Epithelial-Mesenchymal Transition by Atmospheric Pressure Plasma. Front. Phys. 9:694080. doi: 10.3389/fphy.2021.694080

INTRODUCTION

Despite numerous medical therapies to treat cancer, including surgery, chemotherapy, radiation therapy, immunotherapy, cancer is still one of the leading causes of death worldwide [1]. Also, it is known that almost 90% of deaths from cancer are due to cancer metastasis [2,3]. Chemotherapy, indeed, has been studied for the longest and is the most widely used treatment for cancer, but it is still difficult to prevent the dissemination of cancer cells and completely cure cancer because of drug resistance.

In the midst of these difficulties in overcoming cancer, recently, atmospheric pressure plasma (APP) has been suggested for an alternative method for cancer treatment as its action mechanism does not follow the conventional chemotherapy drugs, and instead, various active species (charged particles, UV photons, ROS, NO_X, O_3, etc.) in plasma are known to physically and chemically eradicate cancer cells [4–7]. In addition, in various *in vivo* studies, APP-treatment was shown to impediment tumor growth and improved tumor-implanted animals' survival rate [8,9]. Moreover, growing evidence suggests that cancer cells are more vulnerable to plasma than normal cells [5,6,10]. Along with many of these positive effects, APP treatment is known to be relatively safe because it does not have mutagenic side effects or thermal damage to cells or tissues [7,11,12].

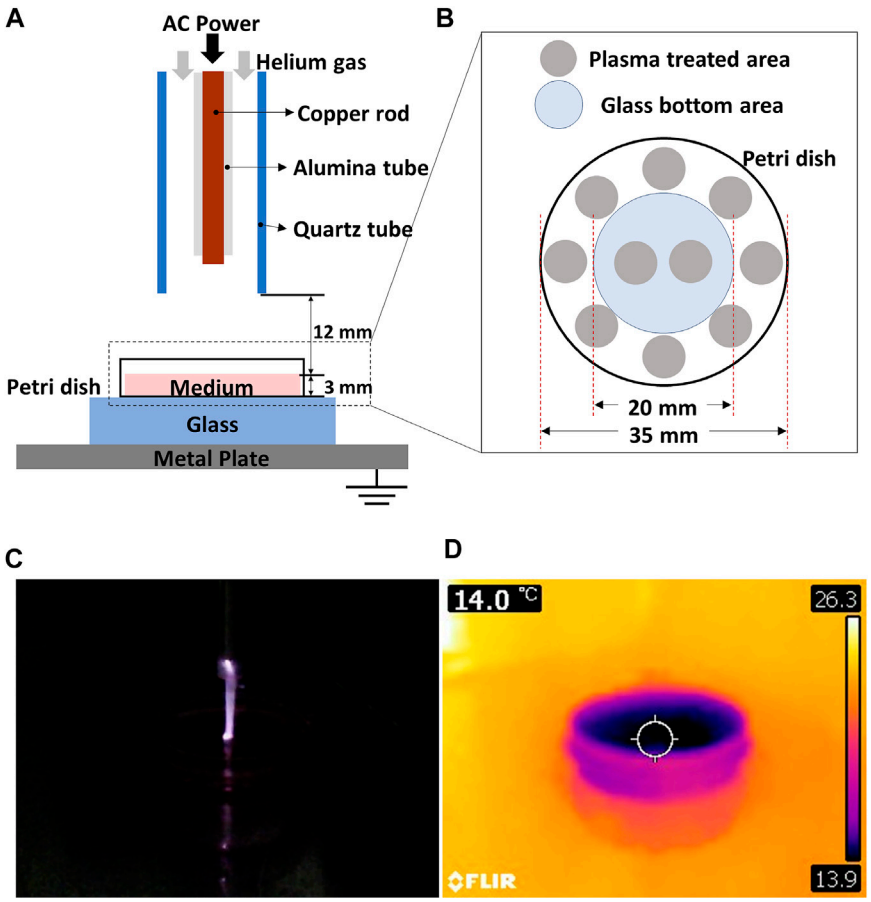

FIGURE 1 | (A) Schematics of a micro-jet atmospheric pressure plasma (APP) treatment system, **(B)** plasma treatment area within the petri dish. **(C)** APP discharge image and **(D)** its thermal image obtained with FLIR C5.

In addition to these direct effects of APP in cancer cells or tumor mass, in our previous studies, we have found the possibility that APP can also be utilized as an auxiliary treatment after cancer surgery. Based on our previous findings that plasma treatment suppresses angiogenesis in endothelial cells [13] and converts the mesenchymal phenotype of mesenchymal cells into epithelial (less motile) phenotype [14], we hypothesized that APP-treatment could further be utilized to inhibit the spread of cancer cells possibly remained after surgery to remote organs. Based on this hypothesis, we treated APP to human breast cancer cells (MDA-MB-231), which is commonly used to establish a metastasis model, and found that plasma treatment can suppress the epithelial-mesenchymal transition (EMT) process and invasion of cells. As EMT and invasion to basement membrane are the key processes of cancer metastasis, we expect that APP treatment can be an effective therapeutic tool to suppress cancer metastasis.

METHODS

Plasma Setup

A micro-jet atmospheric pressure plasma was used for cell treatment. The plasma generator consists of a single copper pin electrode, an alumina tube covering the electrode, and a quartz tube (**Figure 1A**). An alternating current (AC) power supply (FTLab HPSI200) is set to a frequency of 50 kHz, and the peak-to-peak voltage of 2.85 kV (**Supplementary Figure S1**) and helium gas was used to discharge plasma. 4 standard liter per minute (slm) of helium gas was supplied into the tube. In order to ensure that there is no thermal effect induced by plasma, the temperature of the plasma plume was measured with a thermal camera (FLIR C5) and confirmed to be maintained around 14–20°C as shown in **Figures 1C,D**, and **Supplementary Figure S2**.

Cell Culture

The breast cancer cell line, MDA-MB-231, which is known to have a metastatic phenotype, was used in our study. To better observe cells for cell migration and invasion analysis, MDA-MB-231 cells expressing green fluorescent protein (GFP) were used. The cells were cultured using Dulbecco's Modified Eagle's Medium (DMEM, Lonza) mixed 10% fetal bovine serum (FBS, Gibco, NY, United States) and 1% penicillin-streptomycin (Gibco). Cells were maintained in the incubator to provide an optimal environment with a temperature of 37°C, relative humidity of 95%, and 5% CO_2. Cells were prepared on three

different platforms depending on the analysis: 1. 2D imaging for morphology and migration analysis, 2. 3D imaging for 3D migration analysis, and 3. invasion assay. For 2D cell imaging, cells were seeded on collagen I (PureCol, Advanced BioMatrix) coated 35 φ glass-bottom dish (SPL), and for the 3D imaging, cells were seeded on Matrigel (BD Biosciences) coated 35 φ glass-bottom dish. In addition, for invasion assay, cells were seeded on Matrigel-coated 24 φ transwell (Corning) membrane.

Cell Preparation on 2D Matrix, 3D Matrix, and Transwell

To coat collagen-I on a 35 φ glass-bottom dish for 2D culture, collagen-I (100 μg/ml) solution was placed on the glass-bottom dish and kept in 4°C for 12 h. After 12 h, the remained collagen solution on the glass was removed and washed three times. MDA-MB-231 cells were then seeded on the collagen-I coated glass surface at a density of 5,000 cells/cm^2 (**Supplementary Figure S3A**).

To coat Matrigel 35 φ glass-bottom dish for 3D culture, 200 μl of Matrigel mixture were loaded on the glass-bottom dish and kept at room temperature for about an hour. Cells were then seeded at a density of 5,000 cells/cm^2 on the Matrigel (**Supplementary Figure S3B**). After seeding, both on 2D and 3D platforms, cells were incubated for 24 h before the plasma treatment.

For invasion assay, cells were prepared in a transwell. As shown in **Supplementary Figure S3C**, the transwell consists of a cell culture insert and a bottom well. The cell culture insert has a 24 φ polycarbonate membrane with an 8 μm pore. First, we coat the polycarbonate membrane with 200 μl of Matrigel mixture for an hour. Then, cells were seeded at a density of 1.2×10^5 cells/well on the Matrigel surface. Before plasma treatment, cells were kept in the incubator for 24 h. The bottom well needs to be filled with chemoattractant-rich-media (DMEM with 10% FBS) to trigger cell invasion. However, during culture, we used DMEM with 10% FBS in both the cell culture insert and bottom well because we did not want to create a chemo gradient environment across the Matrigel and let cells penetrate it before the plasma treatment.

Plasma Treatment

Right before the plasma treatment, we removed the culture media from the glass-bottom dish (or the transwell) and filled it with fresh FBS-free DMEM. The end of the plasma generator (the end of the quartz tube) was fixed at a distance of 1.2 cm from the surface of the culture medium, filling the glass-bottom dishes or the transwell (**Figure 1A**). Also, to maintain the plasma dosage affecting cells on different cell culture platforms with consistency, the thickness of the culture medium was kept at 3 mm in all three different cell culture platforms (**Figure 1A**). We place a grounded metal plate and a glass plate underneath the glass-bottom dish to let the plasma plume impinging toward the media surface. As the diameter of the plasma jet was approximately 0.5 cm, which is much smaller than the total cell area, we applied plasma on ten different spots as described in **Figure 1B**. Each spot seen in **Figure 1B** was treated one or 2 min; thus, the total treatment time was 10, or 20 min, respectively. In order to keep the plasma treatment points the same for all samples, the points shown in **Figure 1B** were marked on the glass plate placed under the glass-bottom dish. We moved the sample manually every one or 2 min to cover all ten spots.

Cell Invasion Assay

After plasma treatment, the FBS-free-media in the bottom well was replaced with chemoattractant-rich-media, while the FBS-free-medium in cell culture insert was left intact to generate a longitudinal chemo gradient in Matrigel (**Supplementary Figure S3C**). Then, control and plasma-treated cells were incubated in this chemo gradient environment for 72 h before being observed because we tried to allow sufficient time for the cells to reach the bottom of the transwell insert. The detailed experimental schedule is summarized in **Supplementary Figure S4** because the experimental timelines vary depending on the assays and are somewhat complex.

Cell Imaging and Image Analysis

Plasma treated cells culture in a glass-bottom dish (both on 2D and 3D matrices) were incubated for an additional 24 h before being imaged. To quantify morphological traits of cells, we traced cell boundary and measured cell area and aspect ratio using ImageJ software (U.S. National Institutes of Health). The aspect ratio denotes the ratio of the major axis to the minor axis of the ellipses that fits best to the cell shape. For cell migration analysis, phase-contrast images and fluorescence images of cells were taken every 10 min for 12 h using Axiovert 200M (Carl Zeiss) microscope equipped with an incubator and CO_2 controller. From the obtained time-lapse images, cells were manually tracked using a cell tracking plugin in ImageJ software.

As the invading cells travel from the surface of Matrigel through the Matrigel to the bottom of the transwell membrane, we waited 72 h after plasma treatment to image the cells settled down on the bottom of the transwell membrane. FITC filter set (488 nm) and 5x objective lens were used to image GFP expressing cells. For each experimental condition (control, APP 10 min, and APP 20 min), 10 different locations were imaged. The number of cells was then manually counted from the fluorescence images using the cell counting plugin in ImageJ software to evaluate the invasion capacity of MDA-MB-231 cells.

Real-Time PCR

Plasma-treated MDA-MB-231 cells culture in the collagen-I coated glass-bottom dish were incubated for an additional 24 h before being harvested for PCR analysis. Total RNA was obtained from harvested cells with NucleoSpin RNA LL kit (Macherey-Nagel), and cDNA was reversely transcribed from RNA with iScriptTM cDNA synthesis kit (Bio-Rad). iQ SYBR Green supermix (Bio-Rad) and qRT-PCR detection system (Bio-Rad CFX96) were used for real-time PCR. The followings are the primers used in the real-time PCR analysis: Vimentin (forward 5′-TCCCGCATCTCCTCCTCGTA-3′; reverse 3′-CTGAAT GACCGCTTCGCCAA-5′), α-smooth muscle actin (forward 5′-TGACAGGACGTTGTTAGCAT-3′; reverse 3′-GCCATG TATGTGGCTATTCA-5′), NME1 (forward 5′-AAGGAGATC

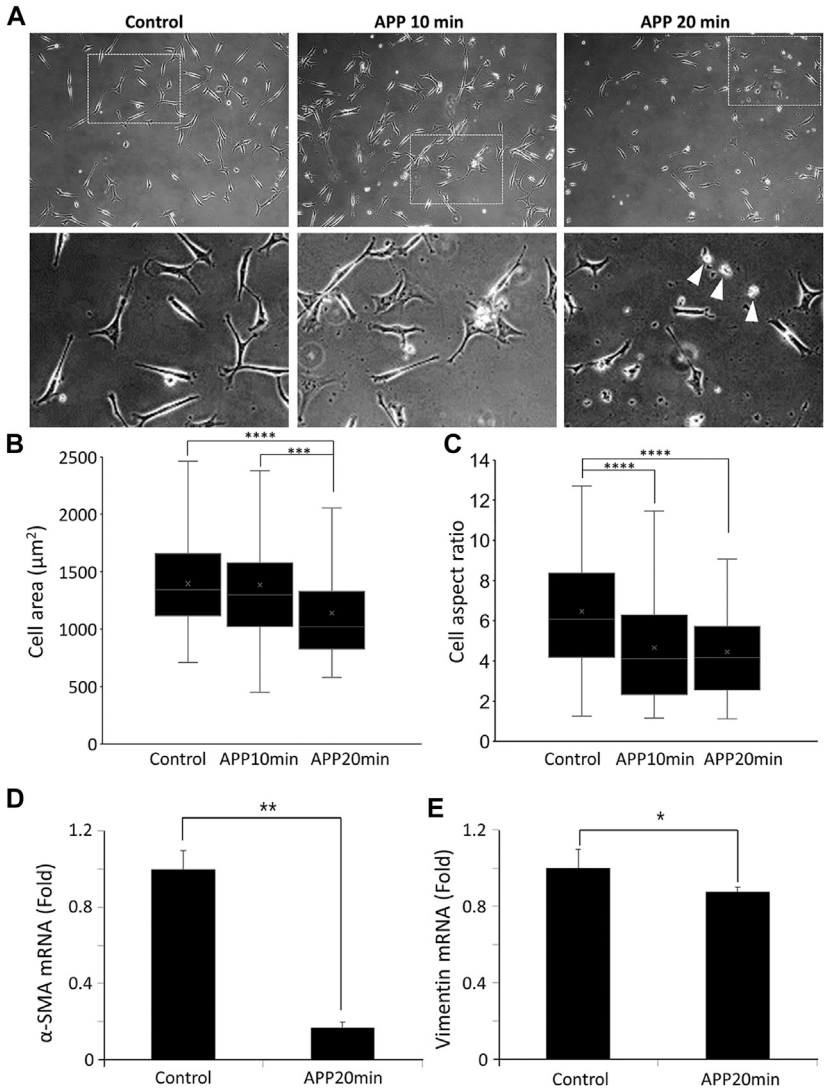

FIGURE 2 | (A) Phase-contrast images of control and 10 min-APP treated, and 20 min-APP treated MDA-MB-231 cells. **(B)** Cell area, and **(C)** aspect ratio of MDA-MB-231 cells (Control $n = 93$, APP 10 min $n = 101$, APP 20 min $n = 91$, ±SD). Relative expression of mesenchymal marker genes; **(D)** α-SMA, and **(E)** Vimentin ($n = 3$, ±SD) $^{*}p < 0.05$, $^{**}p < 0.01$, $^{***}p < 0.001$, and $^{****}p < 0.0001$.

GGCTTGTGGTTT-3′; reverse 3′-CTGAGCACAGCTCGTGTA ATC-5′), KDM3A (forward 5′- GTGCTCACGCTCGGAGAAA-3′; reverse 3′-GTGGGAAACAGCTCGAATGGT-5′) human glyceraldehyde 3-phosphate dehydrogenase (GAPDH; forward 5′-GAAGGTGAAGGTCGGAGTC-3′; reverse 3′-GAAGAT GGTGATGGGATTT-5′).

Immunofluorescence Staining

For immunofluorescence staining, cells were prepared on collagen-I coated glass-bottom dishes. After the plasma treatment, plasma-treated cells and control cells were incubated for another 24 or 48 h, then washed twice with phosphate-buffered saline (PBS, pH 7.4) and fixed with 3.7% formaldehyde/PBS for 15 min at room temperature (RT). After fixing, cells were permeabilized with 0.2% Triton X-100 (Sigma) for 15 min and incubated with 5% BSA/PBS for 1 h at RT. Then, the sample was incubated with the vimentin antibody (ab11256, Abcam) diluted in 1% BSA/PBS overnight at 4°C, and, with the secondary antibody, donkey anti goat alexa fluor 488 (A11055, Invitrogen) for 1 h at RT. To label actin, cells were than incubated with Rhodamine phalloidin (R415, Invitrogen) diluted in PBS for 1 h at RT, and, to label nuclei, cells were incubated with 5 μg/ml Hoechst 33342 (Sigma) diluted in PBS for 10 min at RT. In each step, the sample was washed three times with PBS. For the anti-bleaching method mounting solution (Vectashield® Vector Labs.) was used. Cell images were taken using a widefield fluorescence microscope (DMi8, Leica) and a confocal microscope (TCS SP5, Leica).

Statistical Analysis

To compare the results between the experimental groups (control, APP 10 min, APP 20 min, or gas-treated) unpaired student t-test was conducted using Microsoft Excel and p-values are marked within the graph. ($^{*}p < 0.05$, $^{**}p < 0.01$, $^{***}p < 0.001$, and $^{****}p < 0.0001$).

RESULTS AND DISCUSSION

Alteration in Cell Morphology by Atmospheric Pressure Plasma Treatment

As the plume of plasma did not come into direct contact with the cell layer, we did not observe any necrotic cells immediately after atmospheric pressure plasma (APP) treatment. Also, we did not observe a dramatic decrease in the number of cells in APP-treated group following an additional 24 h of incubation (**Figure 2A**). Interestingly, some round-shaped cells indicating the sign of apoptosis (marked with white arrowheads in **Figure 2A**) appeared in a cell group treated with plasma for 20 min. In many previous reports, APP is known to induce DNA damages and apoptotic cell death [15,16]. Therefore, it was necessary to first determine how plasma affects cell viability before observing other phenotypic changes by APP. We conducted three different assays to more clearly confirm and accurately quantify the effect of plasma on cellular viability: 1) Live/dead assay immediately after the plasma treatment, 2) Annexin-V apoptosis assay 24 h after plasma treatment, and 3) CCK-8 assay across the whole experimental time points (right before the plasma treatment, 24 h after plasma treatment, 48 h after plasma treatment, and 72 h after plasma treatment). The details about the experimental methods and results are described in the Supplementary materials (**Supplementary Figures S4–S7**). Although cellular proliferation rates were slightly affected (decreased by 11–20%), cell viability was not dramatically changed by plasma treatment.

Interestingly, as shown in **Figure 2A**, cellular morphology was slightly altered by APP treatment. Given that no such morphological changes were observed in the gas-treated samples, we confirmed that it was definitely due to APP (**Supplementary Figure S8**). Cell area and aspect ratio were measured to better quantify the morphological changes in cells. MDA-MB-231 cells remained their original elongated shape in the control sample; however, APP-treated cells exhibited a slightly reduced cell area and a rounded and shortened shape rather than an elongated one (**Figures 2B,C**). Morphological alteration became greater with longer APP treatment time, and, especially, the morphological difference was significant between control cells and the cells treated with APP for 20 min (**Figures 2B,C**). Based on these observations, we fixed the APP treatment time at 20 min for a solid comparative study between the control and APP-treated cells.

This morphological change seems to be related to a decrease in the mesenchymal phenotype of cells, we briefly measured the mesenchymal marker genes, alpha smooth muscle actin (α-SMA), and vimentin. In APP-treated cells, as shown in **Figures 2D,E**, mesenchymal marker α-SMA decreased by 80%, and vimentin decreased by 10% compared to the one expressed in control cells. To confirm whether reduction of mesenchymal marker at the mRNA level further induces changes in protein level, we obtained the immunofluorescence images labeled with vimentin.

Alteration of Vimentin by APP Treatment

In the immunofluorescence images, the vimentin architecture seems to be dramatically altered in plasma-treated cells. At an early time point (24 h after plasma treatment), empty spots without vimentin are seen in the cytosolic area (marked with yellow arrowheads in **Figure 3**). In addition, fragmented vimentin was shown in plasma-treated cells (marked with a yellow circle in **Figure 3**), whereas intact vimentin was shown in control cells. Especially, we observed a significant decrease of vimentin in the periphery as indicated by yellow arrowheads in **Supplementary Figure S9**. When this peripheral region was enlarged and observed under a confocal microscope, we could see a more distinct difference between the control and the plasma-treated groups. In control cells, vimentin seems to colocalize with actin filament (white arrowhead in the enlarged images of **Figure 3**), but the decrease of peripheral vimentin in plasma-treated cells seems to reduce the vimentin interacting with actin. Given that vimentin facilitates the migration of cells by incorporating with actin filaments [17–19], it is likely that this reduction in peripheral vimentin may be associated with the reduction in cell migration and invasion. Based on this series of changes, morphological alteration with reduced aspect ratio, reduction of the mesenchymal marker, and loss of peripheral vimentin, we can hypothesize that plasma-induced stress suppressed the epithelial-to-mesenchymal transition (EMT) in cells. To further investigate the functional characteristics associated with EMT, we then investigated the cell migration characteristics of APP-treated cells.

Reduced Cell Migration by APP Treatment

As mentioned in the Methods section above, we have investigated cell migration properties in two different platforms: a 2D matrix using collagen I coated 35 φ glass-bottom dish and a 3D matrix using Matrigel-coated 35 φ glass-bottom dish (See **Supplementary Figures S3A,B**). The representative cell trajectories observed in the 2D matrix are shown in **Figure 4A**. As can be predicted from the 2D trajectory plot, the motility of APP-treated cells drastically decreased (approximately by 88%) compared to one of the control cells (**Figure 4B**).

Considering that cancer cell metastasis requires cells to pass through the basement membranes in the 3D microenvironment, and cell migration characteristics alter when the dimensions of the microenvironment change [20,21], the same migration experiment were repeated in the 3D matrix, Matrigel. As can be seen in **Figure 4C**, the average motility of both control and plasma-treated cells in the 3D matrix was reduced by about 70% compared to the motility in the 2D matrix. Given that cellular motility decreases on the softer substrate, reduction in migration of the cells in the 3D matrix seems to be reasonable because the

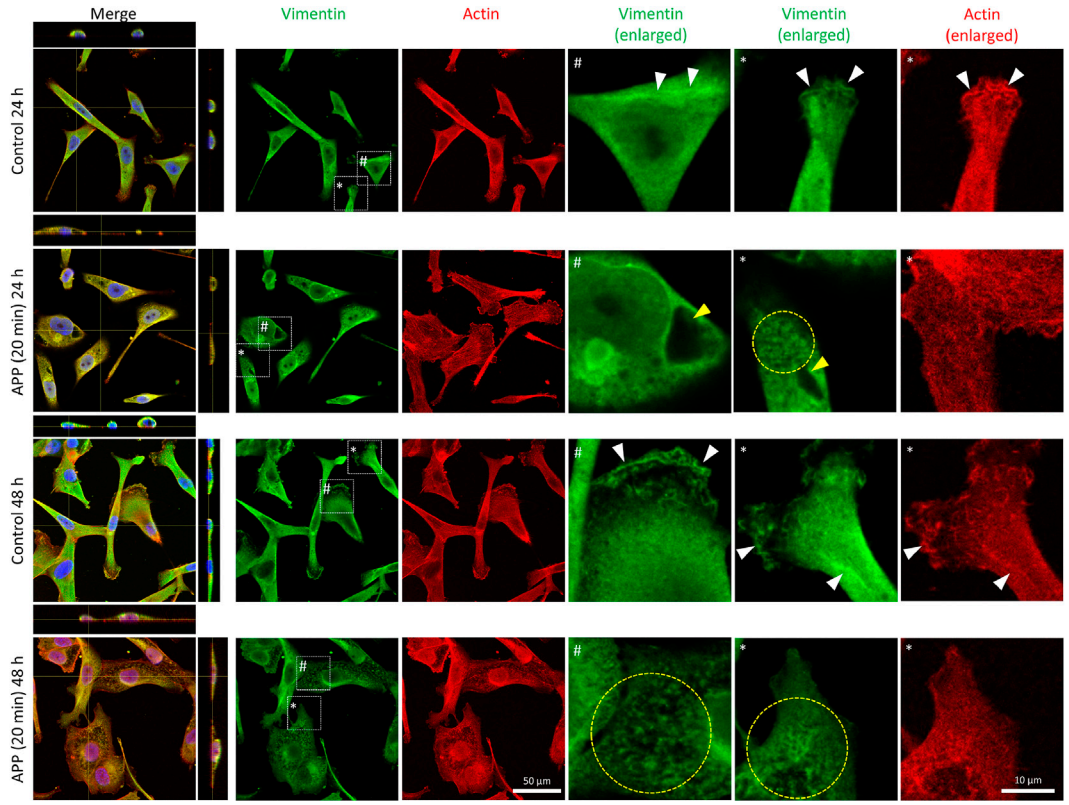

FIGURE 3 | Immunofluorescence images (40x) of control (24 h), 20-min APP (24 h), control (48 h), and 20-min APP (48 h) cells. Vimentin **(green)**, Actin **(red)**, and Nucleus **(blue)**. Scale bar 50 and 10 μm in the enlarged images.

stiffness of Matrigel is known to vary from 0.5 to 10 kPa, whereas the stiffness of glass used in the 2D migration experiment goes up to a few GPa [22–24]. Although overall motility has decreased in the 3D matrix, similar trends are still evident in APP-treated cells. The motility in APP-treated cells dramatically decreased (approximately by 86%) compared to one of the control cells (**Figure 4C**). Although some of the cells on Matrigel could penetrate the gel and make a z-directional motion, only 2D motions of cells within a fixed focal plane were be analyzed because the z-position of the objective lens was fixed during cell imaging.

Suppressed Cell Invasion by APP Treatment

To confirm that the reduced cell migration further impacts cancer cell invasion capacity, we measured cell invasion property through transwell assay. Interestingly but not surprisingly, we found that APP-treated cells tend to invade less than control cells. As shown in **Figure 4D**, far fewer cells successfully reached the bottom of the transwell insert. By 20-min of plasma treatment, cell invasion capacity decreased by 85% (**Figure 4E**). Moreover, just by 10-min plasma treatment, a condition in which the cell's shape did not change significantly, cellular invasion capacity also significantly decreased (71%) (**Figure 4E**). Here, we should be careful when comparing the cell numbers between control and APP-treated cells because the previously shown CCK-8 results show that APP-treatment could suppress cell proliferation (**Supplementary Figure S7**). However, even considering the reduction in cell proliferation rate (maximum 20% drop compared to control), we can assure that the invasion capacity of MDA-MB-231 has decreased because the reduction rate of fully invaded cells was much higher (85% drop compared to control).

As such, atmospheric pressure plasma appears to result in reduced migration, invasion, and possibly suppression of EMT. To further investigate the alterations in the epigenetic markers linked directly to cancer cell invasion and metastasis, we quantified gene expressions of NME1 and KDM3A, which are known to suppress and promote cancer invasion and metastasis, respectively [25–28]. As shown in **Figure 4F**, gene-level expressions of NME1 and KDM3A respectively increased and decreased 48 h after plasma treatment (with a statistical significance in KDM3A expression).

SUMMARY AND FUTURE PERSPECTIVE

Collectively, our study has demonstrated APP-induced alterations in overall cellular morphology and vimentin architecture, whose traits consistently indicated suppression of EMT; this transformation further impacted cellular migration to subdue cancer cell invasion dramatically. Furthermore, these APP-induced phenotypic and functional changes seem to occur with

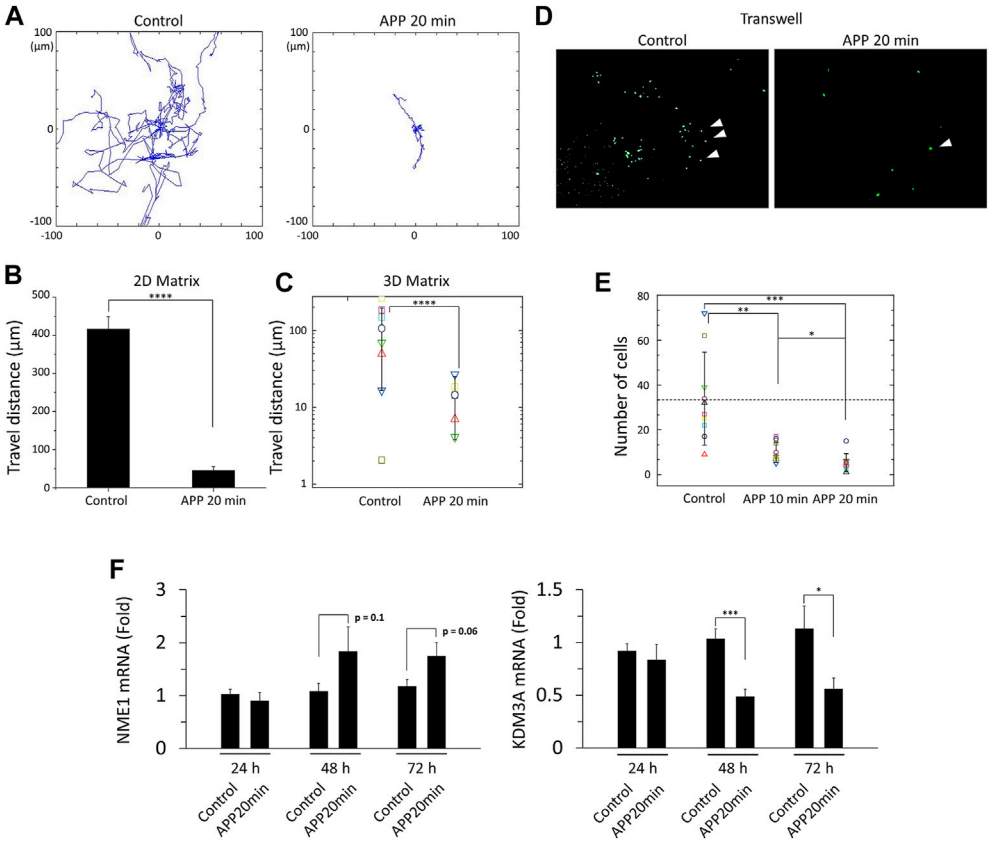

FIGURE 4 | (A) Trajectories of single cells for control and 20 min-APP treated cells. The cells were tracked every 10 min for 12 h. **(B)** Total travel distance of control and 20 min-APP treated cells on the collagen type I coated glass surface, and **(C)** on the Matrigel coated surface (n = 9, ±SD). **(D)** Fluorescence images of the insert bottom (from left to right: control, and 20 min-APP treated MDA-MB-231 cells). **(B)** The number of cells at the insert bottom (n = 10, ±SD). **(F)** Relative mRNA expression of metastasis suppressor NME1, and metastasis promotor KDM3A (n > 8, ±SEM) *p < 0.05, **p < 0.01, ***p < 0.001, and ****p < 0.0001.

more profound epigenetic modifications in NME1 and KDM3A. There has been a great deal of research on development of plasma devices for biomedical research and clinical uses, and the knowledge on its immediate interactions with the cells and tissues are increasingly being accumulated [12,29,30]. Many previous studies focused on the use of APP as a surgical tool to selectively remove cancer cells from the surrounding normal tissues. This study emphasizes the applicability of APP as an auxiliary treatment strategy to inhibit the spread of residual cancer cells remaining after the surgery. Given that metastasis is a highly complicated process that occurs in sequential steps of invasion, intravasation, extravasation, and growth in a secondary organ, further experiments would be necessary to identify the core signaling pathways associated with suppression mechanism of metastasis by APP. Previously, we have identified OH, OI, $N_2^+$and He I peaks in the plasma emission spectrum, which can interact with DMEM to produce reactive species such as hydroxyl radical (•OH), and nitrite (NO_2^-) [31,32]. However, we need to track down the pivotal effectors of APP to have a better control of the anti-metastatic processes.

Over the last 2 decades, studies conducted by various research groups have greatly improved our understanding of the underlying mechanisms of cancer treatment by APP, and through these studies, APP has shown a great potential to become an innovative therapeutic treatment to cure cancer. Given the current level of APP application, it may be difficult for APP to immediately replace the well-established conventional cancer treatment such as surgery or chemotherapy. Therefore, it would be much more realistic to utilize the APP as an auxiliary strategy in parallel with the existing treatment. In this context, we believe that our research has demonstrated a new direction for realizing these applications.

DATA AVAILABILITY STATEMENT

The original contributions presented in the study are included in the article/**Supplementary Material**, further inquiries can be directed to the corresponding authors.

AUTHOR CONTRIBUTIONS

KK, BG, JS, AJ, and WC designed the experiment, and KK, JC, BG, AJ, and UK performed the experiments. KK, BG, and JC analyzed the data. KK, BG, and JS wrote the manuscript. All authors interpreted data, provided critical insights, and edited the manuscript.

FUNDING

This work was supported by the National Research Foundation of Korea (NRF) grant funded by the Korea government (grant numbers: 2020R1F1A1073385).

SUPPLEMENTARY MATERIAL

The Supplementary Material for this article can be found online at: https://www.frontiersin.org/articles/10.3389/fphy.2021.694080/full#supplementary-material

REFERENCES

1. Sung H, Ferlay J, Siegel RL, Laversanne M, Soerjomataram I, Jemal A, et al. Global Cancer Statistics 2020: GLOBOCAN Estimates of Incidence and Mortality Worldwide for 36 Cancers in 185 Countries. *CA A Cancer J Clin* (2021) 71:209–49. doi:10.3322/caac.21660
2. Mehlen P, and Puisieux A. Metastasis: a Question of Life or Death. *Nat Rev Cancer* (2006) 6(6):449–58. doi:10.1038/nrc1886
3. Steeg PS. Targeting Metastasis. *Nat Rev Cancer* (2016) 16(4):201–18. doi:10.1038/nrc.2016.25
4. Fridman G, Shereshevsky A, Jost MM, Brooks AD, Fridman A, Gutsol A, et al. Floating Electrode Dielectric Barrier Discharge Plasma in Air Promoting Apoptotic Behavior in Melanoma Skin Cancer Cell Lines. *Plasma Chem Plasma Process* (2007) 27(2):163–76. doi:10.1007/s11090-007-9048-4
5. Gweon B, Kim M, Kim DB, Kim D, Kim H, Jung H, et al. Differential Responses of Human Liver Cancer and normal Cells to Atmospheric Pressure Plasma. *Appl Phys Lett* (2011) 99(6):063701. doi:10.1063/1.3622631
6. Harley JC, Suchowerska N, and McKenzie DR. Cancer Treatment with Gas Plasma and with Gas Plasma-Activated Liquid: Positives, Potentials and Problems of Clinical Translation. *Biophys Rev* (2020) 12(4):989–1006. doi:10.1007/s12551-020-00743-z
7. Rafiei A, Sohbatzadeh F, Hadavi S, Bekeschus S, Alimohammadi M, and Valadan R. Inhibition of Murine Melanoma Tumor Growth *In Vitro* and *In Vivo* Using an Argon-Based Plasma Jet. *Clin Plasma Med* (2020) 19–20. doi:10.1016/j.cpme.2020.100102
8. Brulle L, Vandamme M, Ries D, Martel E, Robert E, Lerondel S, et al.Effects of a Non Thermal Plasma Treatment Alone or in Combination with Gemcitabine in a MIA PaCa2-Luc Orthotopic Pancreatic Carcinoma Model. *Plos One* (2012) 7(12). doi:10.1371/journal.pone.0052653
9. Walk RM, Snyder JA, Srinivasan P, Kirsch J, Diaz SO, Blanco FC, et al. Cold Atmospheric Plasma for the Ablative Treatment of Neuroblastoma. *J Pediatr Surg* (2013) 48(1):67–73. doi:10.1016/j.jpedsurg.2012.10.020
10. Xiang L, Xu X, Zhang S, Cai D, and Dai X. Cold Atmospheric Plasma Conveys Selectivity on Triple Negative Breast Cancer Cells Both *In Vitro* and *In Vivo*. *Free Radic Biol Med* (2018) 124:205–13. doi:10.1016/j.freeradbiomed.2018.06.001
11. Moon SY, Kim DB, Gweon B, Choe W, Song HP, and Jo C. Feasibility Study of the Sterilization of Pork and Human Skin Surfaces by Atmospheric Pressure Plasmas. *Thin Solid Films* (2009) 517(14):4272–5. doi:10.1016/j.tsf.2009.02.018
12. Wende K, Schmidt A, and Bekeschus S. Safety Aspects of Non-Thermal Plasmas. In: H-R Metelmann, T von Woedtke, and K-D Weltmann, editors. *Comprehensive Clinical Plasma Medicine: Cold Physical Plasma for Medical Application*. Cham: Springer International Publishing (2018). p. 83–109. doi:10.1007/978-3-319-67627-2_5
13. Gweon B, Kim H, Kim K, Kim M, Shim E, Kim S, et al. Suppression of Angiogenesis by Atmospheric Pressure Plasma in Human Aortic Endothelial Cells. *Appl Phys Lett* (2014) 104(13):133701. doi:10.1063/1.4870623
14. Gweon B, Kim M, Kim K, Choung J, Lee MN, Ko UH, et al. Role of Atmospheric Pressure Plasma (APP) in Wound Healing: APP-Induced Antifibrotic Process in Human Dermal Fibroblasts. *Exp Dermatol* (2016) 25(2):159–61. doi:10.1111/exd.12865
15. Guo L, Zhao Y, Liu D, Liu Z, Chen C, Xu R, et al. Cold Atmospheric-Pressure Plasma Induces DNA-Protein Crosslinks through Protein Oxidation. *Free Radic Res* (2018) 52(7):783–98. doi:10.1080/10715762.2018.1471476
16. Gaur N, Kurita H, Oh JS, Miyachika S, Ito M, Mizuno A, et al. On Cold Atmospheric-Pressure Plasma Jet Induced DNA Damage in Cells. *J Phys D-Applied Phys* (2021) 54(3):035203. doi:10.1088/1361-6463/abb8ab
17. Jiu Y, Lehtimäki J, Tojkander S, Cheng F, Jäälinoja H, Liu X, et al. Bidirectional Interplay between Vimentin Intermediate Filaments and Contractile Actin Stress Fibers. *Cel Rep* (2015) 11(10):1511–8. doi:10.1016/j.celrep.2015.05.008
18. Costigliola N, Ding L, Burckhardt CJ, Han SJ, Gutierrez E, Mota A, et al. Vimentin Fibers orient Traction Stress. *Proc Natl Acad Sci USA* (2017) 114(20):5195–200. doi:10.1073/pnas.1614610114
19. Battaglia RA, Delic S, Herrmann H, and Snider NT. Vimentin on the Move: New Developments in Cell Migration, F1000Res. *Vimentin Move: New Developments Cell Migration* F1000res (2018) 7:1796. doi:10.12688/f1000research.15967.1
20. Rowe RG, and Weiss SJ. Breaching the Basement Membrane: Who, when and How?. *Trends Cel Biol* (2008) 18(11):560–74. doi:10.1016/j.tcb.2008.08.007
21. Galarza S, Kim H, Atay N, Peyton SR, and Munson JM. 2D or 3D? How Cell Motility Measurements Are Conserved across Dimensions *In Vitro* and Translate *In Vivo*. *Bioeng Translational Med* (2020) 5(1). doi:10.1002/btm2.10148
22. Discher DE, Janmey P, and Wang YL. Tissue Cells Feel and Respond to the Stiffness of Their Substrate. *Science* (2005) 310(5751):1139–43. doi:10.1126/science.1116995
23. Yeung T, Georges PC, Flanagan LA, Marg B, Ortiz M, Funaki M, et al. Effects of Substrate Stiffness on Cell Morphology, Cytoskeletal Structure, and Adhesion. *Cell Motil. Cytoskeleton* (2005) 60(1):24–34. doi:10.1002/cm.20041
24. Kim M, Gweon B, Koh U, Cho Y, Shin DW, Noh M, et al. Matrix Stiffness Induces Epithelial Mesenchymal Transition Phenotypes of Human Epidermal Keratinocytes on Collagen Coated Two Dimensional Cell Culture. *Biomed Eng Lett* (2015) 5(3):194–202. doi:10.1007/s13534-015-0202-2
25. Smith SC, and Theodorescu D. Learning Therapeutic Lessons from Metastasis Suppressor Proteins. *Nat Rev Cancer* (2009) 9(4):253–64. doi:10.1038/nrc2594
26. Mccorkle JR, Leonard MK, Kraner SD, Blalock EM, Ma DQ, Zimmer SG, et al. The Metastasis Suppressor NME1 Regulates Expression of Genes Linked to Metastasis and Patient Outcome in Melanoma and Breast Carcinoma. *Cancer Genomics & Proteomics* (2014) 11(4):175–94.
27. Liu J, Liang T, and Zhangsun W. KDM3A Is Associated with Tumor Metastasis and Modulates Colorectal Cancer Cell Migration and Invasion. *Int J Biol Macromolecules* (2019) 126:318–25. doi:10.1016/j.ijbiomac.2018.12.105
28. Liu J, Li D, Zhang X, Li Y, and Ou J. Histone Demethylase KDM3A Promotes Cervical Cancer Malignancy through the ETS1/KIF14/Hedgehog Axis. *Ott* (2020) Vol. 13:11957–73. doi:10.2147/Ott.S276559
29. Metelmann H-R, Seebauer C, Miller V, Fridman A, Bauer G, Graves DB, et al. Clinical Experience with Cold Plasma in the Treatment of Locally Advanced Head and Neck Cancer. *Clin Plasma Med* (2018) 9:6–13. doi:10.1016/j.cpme.2017.09.001
30. Reuter S, von Woedtke T, and Weltmann KD. The kINPen-A Review on Physics and Chemistry of the Atmospheric Pressure Plasma Jet and its Applications. *J Phys D-Applied Phys* (2018) 51(23). doi:10.1088/1361-6463/aab3ad
31. Gweon B, Kim D, Kim DB, Jung H, Choe W, and Shin JH. Plasma Effects on Subcellular Structures. *Appl Phys Lett* (2010) 96(10):101501. doi:10.1063/1.3352316
32. Park JY, Park S, Choe W, Yong HI, Jo C, and Kim K. Plasma-Functionalized Solution: A Potent Antimicrobial Agent for Biomedical Applications from Antibacterial Therapeutics to Biomaterial Surface Engineering. *ACS Appl Mater Inter* (2017) 9(50):43470–7. doi:10.1021/acsami.7b14276

Conflict of Interest: The authors declare that the research was conducted in the absence of any commercial or financial relationships that could be construed as a potential conflict of interest.